



Radiometric calibration of the in-flight blackbody calibration system

C. Monte et al.

Radiometric calibration of the in-flight blackbody calibration system of the GLORIA interferometer

C. Monte¹, B. Gutschwager¹, A. Adibekyan¹, M. Kehrt¹, A. Ebersoldt², F. Olschewski³, and J. Hollandt¹

¹Physikalisch-Technische Bundesanstalt, Abbestraße 2–12, 10587 Berlin, Germany

²Karlsruhe Institute of Technology, 76344 Eggenstein-Leopoldshafen, Germany

³University of Wuppertal, Atmospheric Physics, 42119 Wuppertal, Germany

Received: 15 May 2013 – Accepted: 21 May 2013 – Published: 14 June 2013

Correspondence to: J. Hollandt (joerg.hollandt@ptb.de)

Published by Copernicus Publications on behalf of the European Geosciences Union.

Title Page

Abstract

Introduction

Conclusions

References

Tables

Figures



Back

Close

Full Screen / Esc

Printer-friendly Version

Interactive Discussion



Abstract

GLORIA is an airborne, imaging, infrared Fourier transform spectrometer that applies the limb-imaging technique to perform trace gas and temperature measurements in the Earth's atmosphere with 3-dimensional resolution. To ensure the traceability of these measurements to the International Temperature Scale and thereby to an absolute radiance scale, GLORIA carries an on-board calibration system. It basically consists of two identical large area and high emissivity infrared radiators, which can be continuously and independently operated at two adjustable temperatures in a range from -50°C to 0°C during flight. Here we describe the radiometric and thermometric characterization and calibration of the in-flight calibration system at the Reduced Background Calibration Facility of the Physikalisch-Technische Bundesanstalt with a standard uncertainty of less than 100 mK. Extensive investigations of the system concerning its absolute radiation temperature and spectral radiance, its temperature homogeneity and its short- and long-term stability are discussed. The traceability chain of these measurements is presented.

1 Introduction

The Gimballed Limb Observer for Radiance Imaging of the Atmosphere (GLORIA) (Friedl-Vallon et al., 2013; Riese et al., 2013) is an airborne imaging Fourier Transform Spectrometer (FTS) that utilizes the infrared limb-imaging technique to provide trace gas measurements in the Upper Troposphere/Lower Stratosphere (UTLS) region with unrivalled 3-dimensional spatial resolution. The highly dynamic structure and chemical composition of the UTLS play an essential role in the Earth's climate system, causing prominent changes in the surface temperature via changes in the atmospheric radiative forcing (Solomon et al., 2010; Riese et al., 2012). To ensure traceable and sufficiently accurate measurements of the crucial parameters, i.e. atmospheric temperature and trace gas distributions, GLORIA applies a sophisticated in-flight blackbody calibration

AMTD

6, 5251–5295, 2013

Radiometric calibration of the in-flight blackbody calibration system

C. Monte et al.

Title Page

Abstract

Introduction

Conclusions

References

Tables

Figures

⏪

⏩

◀

▶

Back

Close

Full Screen / Esc

Printer-friendly Version

Interactive Discussion

Radiometric calibration of the in-flight blackbody calibration system

C. Monte et al.

Title Page

Abstract

Introduction

Conclusions

References

Tables

Figures

⏪

⏩

◀

▶

Back

Close

Full Screen / Esc

Printer-friendly Version

Interactive Discussion



in December 2011. GLORIA has been in particular developed for operation in the belly pod of the new German research aircraft, the High Altitude and LOng Range Research Aircraft (HALO), and successfully completed its first scientific deployment during the TACS/ESMVal Campaign (Transport and Composition in the UTLS/Earth System Model Validation) on HALO in September 2012. Several HALO campaigns will follow and further Geophysica campaigns will be proposed at EU level.

The GLORIA instrument and its scientific capabilities are described in detail in Friedl-Vallon et al. (2013); Riese et al. (2013). In brief, a two-lens aspherical optics system is used to image the actual atmospheric conditions via an FTS on a 2-dimensional detector array for detailed infrared limb observations in emission. The detector array consists of 128×128 single detector elements providing over 16 000 simultaneous spectrally resolved limb views in a spectral range from 770 cm^{-1} to 1400 cm^{-1} ($13 \mu\text{m}$ to $7 \mu\text{m}$). The gimbal mount, which stabilizes the line-of-sight during flight, also allows for pointing at azimuth angles between 45° and 135° with respect to the flight direction, as well as Nadir viewing. GLORIA delivers images of the atmospheric limb, within a field-of-view of $4.07^\circ \times 4.07^\circ$, which extends from tangent altitudes of 4 km to about flight level. The gimbal ability is also used to regularly align the FTS with its in-flight calibration sources.

Further to the required 1 % uncertainty in the absolute knowledge of the GLORIA spectral responsivity, the specific data evaluation procedure of limb sounding requires an uncertainty for the relative responsivity of adjacent lines of pixels on the detectors of even 0.1 %. This implies strong demands on the radiance homogeneity of the GBBs and their spatially resolved calibration. Above all GLORIA served as the proof of concept for the InfraRed Limb Sounder of PREMIER (PRocess Exploitation through Measurements of Infrared and Millimetre-wave Emitted Radiation), which has been one of ESA's candidate Earth Explorer Core Missions (ESA, 2008).

2.2 The GLORIA calibration system

The GLORIA calibration system has been designed, built and laboratory tested by the Department of Atmospheric Physics at the University of Wuppertal, Germany. Its

Radiometric calibration of the in-flight blackbody calibration system

C. Monte et al.

Title Page

Abstract

Introduction

Conclusions

References

Tables

Figures

⏪

⏩

◀

▶

Back

Close

Full Screen / Esc

Printer-friendly Version

Interactive Discussion



control electronics were developed and built by the Institute for Data Processing and Electronics of Karlsruhe Institute of Technology. The design and thermal performance of the calibration system is described in detail in Olschewski et al. (2013). Throughout the deployment of GLORIA in the ESSenCe and TACS/ESMVal campaigns, the GBBs have been successfully operated and applied for calibration.

The actual range of reference temperatures for the two-point calibration of GLORIA has been established in an optimization process under ideal metrological aspects and practical considerations of its technical realization during flight. An ideal measurement of the detector offset, which is generated by the instrument's self-emission, would require a "zero-emission" source, which is a source at 0 K. However, in practice a reference temperature below ambient temperature bears the risk of water or ice building on the emitting surface and thus significantly changing the surface temperature and emissivity. To frame the radiance levels that occur during measurements in the UTLS and to define temperatures which are practically feasible within reasonable operating times, the range of reference temperatures was fixed to at least 10 K below and 30 K above ambient temperature, i.e. the temperature of the GLORIA instrument compartment. The temperatures inside the instrument compartment are typically 20 K to 30 K above the temperature outside the airplane. In the UTLS this results in reference temperatures in the range from about -50°C to 0°C for the cold (GBB-C) and the warm (GBB-H) GLORIA blackbody.

The major radiometric and thermometric requirements on the GLORIA calibration system (Olschewski et al., 2013) are summarized as follows:

- Minimum size of radiating area $102\text{ mm} \times 102\text{ mm}$.
- Temperature of the GBB-C at least 10 K below ambient temperature.
- Temperature difference between the GBB-C and GBB-H at least 40 K.
- Standard uncertainty of surface radiation temperature less than 100 mK.
- Short-term temperature stability better than 25 mK min^{-1} .

Radiometric calibration of the in-flight blackbody calibration system

C. Monte et al.

Title Page

Abstract

Introduction

Conclusions

References

Tables

Figures

⏪

⏩

◀

▶

Back

Close

Full Screen / Esc

Printer-friendly Version

Interactive Discussion

- Temperature homogeneity better than 150 mK over full aperture.

The limited resources in weight and electrical power provided in the instrument compartment of the aircraft, the harsh and rapidly changing environmental conditions during flight and the demanding calibration requirements of GLORIA meant a major challenge for the design and operation of the calibration system.

The concept of one of the two identical GBBs is shown in Fig. 3. The radiating optical surface of a GBB spans 126 mm × 126 mm and consists of an array of 7 × 7 single pyramids made of aluminium. The pyramids as well as the casing are varnished with NEXTEL Velvet Coating 811-21 yielding a surface emissivity of 0.967 in the range from 5 μm to 12 μm (Lohrengel and Todtenhaupt, 1996). To avoid direct reflections by surfaces perpendicular to the line of sight, three types of pyramids are used with different square bases at different height levels. Thus light traps are formed at the bottom of the pyramids to prevent direct back reflections. Calculations of the geometry factors of the pyramid array in a medium-sized box according to Howell (2010) and their weighting with the surface emissivity of the NEXTEL coating resulted in an effective emissivity of the GBBs of 0.9996 (Olschewski et al., 2013).

For temperature monitoring and control of the GLORIA calibration system, each GBB is equipped with 24 Platinum Resistance Thermometers (PRTs) of the type DIN B/10 (100 Ω) with a nominal temperature uncertainty of 30 mK at 0 °C. Five pyramids of each GBB radiating optical surface are equipped with a PRT close to the apex and another PRT close to the base, respectively. Figure 4 illustrates that these pyramids are positioned close to the corners and in the centre of the pyramid array. During operation individual temperature control in four sectors of the optical surface is performed with the mean value of the apex and the base temperature of the respective corner pyramid as the control value. Fourteen more PRTs are used for monitoring the temperatures of the casing and the cooling surfaces of each GBB.

Operating the GBBs at temperatures below and above ambient temperature is achieved by Thermo-Electric Coolers (TECs) which provide the options of cooling and heating by simply switching the direction of the electrical current. For the temperature

control of the radiating optical surface, an assembly of four two-stage TECs (type Peltron 128A0020) is used with each GBB. Two TECs (type Peltron 128A2427) are used to cool the casing and the baffle system, respectively (Fig. 3).

Both GBBs are suspended to the GLORIA instrument by glass-fibre-reinforced plastic tubes for thermal decoupling and are covered with polystyrene foam sheets to reduce the thermal influence of the environment.

2.3 The reduced background calibration facility

The RBCF of PTB serves as a facility for the measurement of spectral radiance and radiation temperature of radiation sources and the signal-temperature characteristic of radiation thermometers under reduced infrared background radiation in a temperature range from $-170\text{ }^{\circ}\text{C}$ to $430\text{ }^{\circ}\text{C}$ traceable to the ITS-90. Furthermore, it allows the spectrally and angularly resolved measurement of the spectral emissivity of samples from $-40\text{ }^{\circ}\text{C}$ to $600\text{ }^{\circ}\text{C}$. Measurements can be performed in air, under the pressure conditions of the upper atmosphere, and in vacuum.

2.3.1 Set-up and calibration procedure

The set-up of the RBCF and its radiometric application for source and detector calibrations as well as emissivity measurements are described in detail in Monte et al. (2009a,b). Its major vacuum components are: a source chamber, accommodating the blackbody reference radiators, an opto-mechanical unit, allowing folding mirrors and an optical chopper to be inserted into the line of sight, a beam line and a detector chamber, which houses the Vacuum InfraRed Standard radiation Thermometer (VIRST). Additionally, an off-axis ellipsoidal mirror in the detector chamber allows the guiding of the radiation from the source chamber into a vacuum FTS for spectrally resolved measurements (Fig. 5). All optical baffles, the gold-coated folding mirrors and chopper, and the walls of the beam line are cooled by means of liquid nitrogen to temperatures below $-150\text{ }^{\circ}\text{C}$.

Radiometric calibration of the in-flight blackbody calibration system

C. Monte et al.

Title Page

Abstract

Introduction

Conclusions

References

Tables

Figures



Back

Close

Full Screen / Esc

Printer-friendly Version

Interactive Discussion



limits the sensitive spectral range from 8 μm to 14 μm . VIRST achieves a temperature resolution (NETD) of better than 10 mK at 0°C.

The vacuum FTS is a commercial system of the type BRUKER VERTEX 80v which allows for spectrally resolved measurements from 0.4 μm to 1400 μm . For high stability the system applies a linear air-bearing scanner and has been additionally temperature stabilized to better than 100 mK.

For the characterization and calibration of the GBBs, two measurement schemes have been applied:

- Using VIRST, radiation temperatures of the optical surface from -50°C to 0°C have been measured in temperature steps of 5°C by direct comparison to the radiation temperature of the VLTBB. These measurements provide the calibration of the radiation temperature-resistance-characteristics of the GLORIA BB PRTs. The field-of-view of VIRST on the optical surface of the GBBs is 10 mm in diameter. With VIRST spatially resolved temperature measurements have been performed over the full aperture of the optical surface. In addition, VIRST measured the short-term stability of the GBBs.
- Using the vacuum FTS, spectrally resolved radiance measurements of the optical surface have been performed from 7 μm to 16 μm by direct comparison to the spectral radiance of the VLTBB. The field-of-view of the vacuum FTS on the optical surface of the GBBs is 18 mm in diameter. Measurements have been performed at -50°C and 0°C for the three different pyramid types on the optical surface.

So far three calibration campaigns have been performed with the GBBs at the RBCF: in December 2010 about one year before the maiden flight of GLORIA, in January 2012 shortly after its successful test flight with the Geophysica during the ESA Sounder Campaign ESSenCe, and in January 2013 about four months after its first scientific campaign with HALO during the TACS/ESMVal Campaign.

Radiometric calibration of the in-flight blackbody calibration system

C. Monte et al.

Title Page

Abstract

Introduction

Conclusions

References

Tables

Figures



Back

Close

Full Screen / Esc

Printer-friendly Version

Interactive Discussion



2.3.2 Traceability chain and uncertainty

The calibration of the GBBs is traceable to the VLTBB, which is a calibration standard of radiation temperature and spectral radiance and is linked to the ITS-90 via its calibrated PRTs (Fig. 7). The design, thermal performance and effective emissivity of the VLTBB are described in detail in Morozova et al. (2008). In brief, the VLTBB consists of a cavity with three heat-links, three independently controlled electrical heating zones along the cavity, 13 PRTs, a cryo-shroud with a heat-exchanger operating with liquid nitrogen, an electrical heater around the cryo-shroud and two successive radiation shields (Fig. 8). The cylindrical cavity is made of oxygen-free copper, 40 mm in diameter, 250.6 mm in length with a conical bottom and coated with black Aeroglaze Z306. The surface temperature of the cavity is monitored with 9 PRTs selected for stability and calibrated traceable to the ITS-90 at PTB, while 4 fast-response PRTs are used to control the cavity and shroud temperature.

The basic parameters and performance of the VLTBB, as derived from measurements, are given in Table 1 (Morozova et al., 2008; Monte et al., 2013).

The uncertainty budget of the VLTBB is given in Tables 2 and 3. It is based on the uncertainty of the PRT temperature measurement and the uncertainty of the non-isothermal effective cavity emissivity. PRT temperature uncertainties include the PRT calibration uncertainty at PTB traceable to ITS-90, the stability of calibration over time, and the type A uncertainty of PRT temperature measurement during comparison measurements with the VLTBB (JCGM, 2008). For the uncertainty of the effective cavity emissivity, the emissivity of the cavity wall coating has been measured at PTB (Monte and Hollandt, 2010a,b). Additionally, the non-isothermality along the cavity wall has been measured by PRTs for all relevant temperatures of the VLTBB. Isothermal and non-isothermal effective cavity emissivities have been calculated with the blackbody emissivity modelling program STEEP 3 (Prokhorov, 1998, 2013). STEEP calculations have been performed for the observation geometry of VIRST over the relevant wavelength range of the GBBs.

Radiometric calibration of the in-flight blackbody calibration system

C. Monte et al.

Title Page

Abstract

Introduction

Conclusions

References

Tables

Figures



Back

Close

Full Screen / Esc

Printer-friendly Version

Interactive Discussion



Radiometric calibration of the in-flight blackbody calibration system

C. Monte et al.

Title Page

Abstract

Introduction

Conclusions

References

Tables

Figures



Back

Close

Full Screen / Esc

Printer-friendly Version

Interactive Discussion



comparison. A modified optics system of the radiation thermometer allowed viewing the VLTBB directly, without using a window, by attaching it to the opto-mechanical unit of the RBCF via an adjustable vacuum flange. The comparison was performed over the temperature range from -40°C to 50°C and showed an agreement of both blackbodies ranging from a 43 mK deviation at 50°C to a 209 mK deviation at -40°C . Thus both blackbodies agree well within the rather large extended uncertainty of this comparison. The uncertainty of this comparison, ranging from 150 mK at 50°C to 400 mK at -40°C , was mainly caused by the comparison instrument and the comparison procedure. Due to the fact that a blackbody operated under vacuum is compared to a blackbody operated in air, several corrections had to be performed in the comparison process. For this reason, the main contributions to the uncertainty of the comparison are: the correction of the size-of-source effect of the radiation thermometer due to the different temperature environments of the blackbodies, the correction of atmospheric absorption when viewing the ammonia heat-pipe blackbody in air, the correction for changes of the internal temperature of the radiation thermometer, and the correction for a sensitivity drift of the radiation thermometer. To carefully perform these corrections, the size-of-source effect and the temperature parameter of the radiation thermometer have been determined. Possible drifts of the radiation thermometer were corrected by measuring the VLTBB between two measurements at the ammonia heat-pipe blackbody. However, the performance of the compact industrial radiation thermometer clearly limited the achievable comparison uncertainty, especially at lower temperatures. In this context it should be pointed out that the original purpose and proper task of this radiation thermometer, which is easy to transport and operate, is to enable a simple and fast comparison of the blackbodies in the RBCF with the ammonia heat-pipe blackbody near room temperature in order to detect possible long-term drifts of the PRTs of the vacuum blackbodies and help to define their recalibration intervals; a task it performs very well.

3 Calibration results

During three calibration campaigns the GBBs have been comprehensively characterized at the RBCF in the period from December 2010 to January 2013 in terms of their radiometric and thermometric requirements summarized in Sect. 2.2.

3.1 Radiation temperature calibration of PRTs

For the calibration of the radiation temperature versus resistance characteristics of all 10 PRTs of each GBB the temperature of the GBB was changed from -50°C to 0°C in steps of 5°C . For each temperature VIRST measured the radiation temperature of the optical surface at the position of the corresponding PRT while simultaneously the resistance values of the PRT were recorded. The resulting calibration points of each PRT were fitted with a fourth-power polynomial, yielding the calibration characteristic for the corresponding thermometer during the successive GBB operation in flight. In Fig. 12 two typical calibration results are presented where the deviations of the measured radiation temperatures from the calibration curve at the corresponding resistances of the PRTs (i.e. the residuals of the fit) including the uncertainty of each measurement are shown. In Table 4 the maximum individual deviation of a calibration point from the fitted polynomial for each PRT during the January 2013 calibration campaign and the corresponding uncertainty is given. In all cases the deviations can be neglected with respect to the calibration uncertainty. In general the standard calibration uncertainty resulting from this procedure is always less than 110 mK for all PRTs and all temperatures and therefore reliably fulfills the calibration uncertainty requirements of the GBBs.

3.2 Short-term stability

The short-term stability of both GBBs has been measured with VIRST at several temperatures and several positions on their optical surface. All measurements confirmed

Radiometric calibration of the in-flight blackbody calibration system

C. Monte et al.

Title Page

Abstract

Introduction

Conclusions

References

Tables

Figures

◀

▶

◀

▶

Back

Close

Full Screen / Esc

Printer-friendly Version

Interactive Discussion

that the required stability of better than 25 mK min^{-1} is achieved. Examples are given in Figs. 13 and 14.

3.3 Temperature homogeneity

The temperature homogeneity of both GBBs across their optical surface has been measured at several temperatures by scanning the GBBs in two dimensions through the field-of-view of VIRST. The two-dimensional scans were performed as a 9×9 grid with 9 mm step size matched to the 10 mm diameter of the field-of-view of VIRST. All measurements confirmed that the required homogeneity of better than 150 mK over the full optical surface is achieved. Examples are given in Figs. 15 to 17. Herein the data recorded within the circular field-of-view of VIRST are depicted as full squares (left panels). For a better visualization the measured data are also shown as spline interpolated values on a 91×91 grid.

3.4 Spectral radiance

The spectrally resolved radiation temperature of both GBBs has been measured with the vacuum FTS at several temperatures and several positions of their optical surface over the full operating spectral range of GLORIA and beyond. The 18 mm diameter field-of-view of the vacuum FTS was placed at several positions of the optical surface, considering that all three different types of pyramids were alternatively observed (compare insets Figs. 18 and 19). The measured radiation temperatures showed no significant dependence on wavelength or surface position. All measurements confirmed that a high as well as spatially and spectrally homogeneous effective emissivity is achieved with the coated pyramid array. Examples are given in Figs. 18 and 19.

The semitransparent areas in Figs. 18 and 19 illustrate the ranges of the combined standard uncertainty of the spectral distribution of the radiation temperatures determined at three positions of the optical surface. The uncertainty of the radiation temperature results from four contributions: the temperature stability of the GBB-H during the

Radiometric calibration of the in-flight blackbody calibration system

C. Monte et al.

Title Page

Abstract

Introduction

Conclusions

References

Tables

Figures

⏪

⏩

◀

▶

Back

Close

Full Screen / Esc

Printer-friendly Version

Interactive Discussion



measurement, the homogeneity of the radiation temperature within each of the three measurement areas of the spectrally resolved measurement, the spectrally dependent uncertainty of the reference blackbody VLTBB as given in Table 3 and the type A uncertainty of the spectrometer measurements. The latter two dominate the combined uncertainty.

3.5 Long-term stability

The short-term stability of the radiation temperature versus resistance characteristics of all PRTs of the GBBs during laboratory calibration at the RBCF was checked several times during all three calibration campaigns and was insignificant, i.e. stayed well below the calibration uncertainty. However, special care was taken to check the stability of all PRTs before and after flight operation. Therefore the resulting fourth-power polynomials fitted to the calibration points before and after flight operation were compared for each PRT and the maximum deviation before and after flight recorded. Figure 20 gives two examples of PRT calibration curves before and after flight operation. Table 5 gives the maximum individual change of the fitted calibration characteristics for each PRT resulting from the January 2012 and January 2013 calibration campaigns, i.e. before and after GLORIA first scientific campaign with HALO during the TACS/ESMVal Campaign. The PRTs are grouped into two stability categories, representing the requirements: better than 1 % and better than 3 % of spectral radiance uncertainty corresponding to 170 mK and 500 mK radiation temperature uncertainty over the full spectral range of the GBBs. Table 5 reveals that the stability of the radiation temperature-versus-resistance characteristics of the PRTs under the rough environment during flight operation is the major uncertainty contribution in the traceability of the GBBs to the ITS-90. To quantify and minimize this effect, contemporary calibrations of all PRTs before and after flight operation are necessary.

Radiometric calibration of the in-flight blackbody calibration system

C. Monte et al.

Title Page

Abstract

Introduction

Conclusions

References

Tables

Figures



Back

Close

Full Screen / Esc

Printer-friendly Version

Interactive Discussion

4 Summary and outlook

To ensure the traceability of the trace gas and temperature measurements of the airborne limb sounding experiment GLORIA to the International Temperature Scale and thereby to an absolute radiance scale, GLORIA carries an on-board calibration system.

It basically consists of two identical large area and high emissivity infrared radiators, which can be continuously and independently operated at two adjustable temperatures in a range from -50°C to 0°C during flight. We described the thorough radiometric and thermometric characterization and calibration of the in-flight calibration system at the Reduced Background Calibration Facility of the Physikalisch-Technische Bundesanstalt during three calibration campaigns before and after flight of the GLORIA instrument. The radiation temperature versus resistance characteristics of all 10 PRTs of each GBB have been calibrated with a standard uncertainty less than 110 mK for all PRTs and all relevant temperatures and therefore reliably fulfil the calibration uncertainty requirements of the GBBs. All measurements confirmed that the required short-term stability of better than 25 mK min^{-1} and spatial homogeneity of better than $\pm 75\text{ mK}$ over the full optical surface is achieved by both GBBs. The measured radiation temperatures showed no significant dependence on wavelength or surface position. All measurements confirmed that a high as well as spatially and spectrally homogeneous effective emissivity is achieved with the coated pyramid array. The GLORIA calibration system will be regularly linked to the ITS-90 via the Reduced Background Calibration Facility at PTB to provide traceability of the GLORIA atmospheric measurements as needed.

The achieved spatial temperature homogeneity, which fully complies with the requirements, can be further improved by modifying the temperature control software. Although four independent TEC control circuits for the four sectors of the pyramid array are already implemented, currently only one single temperature set point value for all four sectors is freely selectable. Performance can further be improved by reducing the thermal mass of the optical surface. A new design of the pyramid array with an

Radiometric calibration of the in-flight blackbody calibration system

C. Monte et al.

Title Page

Abstract

Introduction

Conclusions

References

Tables

Figures



Back

Close

Full Screen / Esc

Printer-friendly Version

Interactive Discussion

Radiometric calibration of the in-flight blackbody calibration system

C. Monte et al.

Title Page

Abstract

Introduction

Conclusions

References

Tables

Figures

⏪

⏩

◀

▶

Back

Close

Full Screen / Esc

Printer-friendly Version

Interactive Discussion



Gutschwager, B., Theocharous, E., Monte, C., Adibekyan, A., Reiniger, M., Fox, N. P., and Hollandt, J.: Comparison of the radiation temperature scales of the PTB and the NPL in the temperature range from -57°C to 50°C , *Measurement Science and Technology*, 24, 065002.1–065002.9, 2013. 5262

5 Hollandt, J., Friedrich, R., Gutschwager, B., Taubert, D. R., and Hartmann, J.: High-accuracy radiation thermometry at the National Metrology Institute of Germany, the PTB, High Temperatures – High Pressures, 35/36, 379–415, 2003/2007. 5262

Howell, J. R.: A catalog of radiation heat transfer configuration factors, available at: <http://www.engr.uky.edu/rtl/Catalog/> (last access: May 2013), 2010. 5257

10 Joint Committee for Guides in Metrology (JCGM): Evaluation of measurement data – Guide to the expression of uncertainty in measurement, BIPM, 2008. 5261

Lohrengel, J. and Todtenhaupt, R.: Wärmeleitfähigkeit, Gesamtemissionsgrade und spektrale Emissionsgrade der Beschichtung Nextel-Velvet-Coating 811-21 (RAL 900 15 tiefschwarz matt), *PTB-Mitteilungen*, 106, 259–265, 1996. 5257

15 Monte, C. and Hollandt, J.: The determination of the uncertainties of spectral emissivity measurements in air at the PTB, *Metrologia*, 47, S172–S181, 2010a. 5261

Monte, C. and Hollandt, J.: The Measurement of Directional Spectral Emissivity in the Temperature Range from 80°C to 400°C at the Physikalisch-Technische Bundesanstalt, *High Temp. – High Press.*, 39, 151–164, 2010b. 5261

20 Monte, C., Gutschwager, B., and Hollandt, J.: The Reduced Background Calibration Facility for Detectors and Radiators at the Physikalisch-Technische Bundesanstalt, in: *Sensors, Systems, and Next-Generation Satellites XIII*, edited by: Meynart, R., Neeck, S. P., and Shimoda, H., Vol. 7474, *Proceedings of SPIE/*, 747414, Berlin, 2009a. 5254, 5258

Monte, C., Gutschwager, B., Morozova, S., and Hollandt, J.: Radiation Thermometry and Emissivity Measurements under Vacuum at the PTB, *Int. J. Thermophys.*, 30, 203–219, 2009b. 5254, 5258

Monte, C., Gutschwager, B., Adibekyan, A., Kehrt, M., Olschewski, F., and Hollandt, J.: Radiation Thermometry for Remote Sensing at PTB, in: *Proceedings 9th International Temperature Symposium (ITS-9)*, 2013. 5259, 5261, 5262

30 Morozova, S., Parfentiev, N., Lisiansky, B. E., Sapritsky, V. I., Dovgilov, N. L., Melenevsky, U. A., Gutschwager, B., Monte, C., and Hollandt, J.: Vacuum Variable Temperature Blackbody VLTBB100, *Int. J. Thermophys.*, 29, 341–351, 2008. 5259, 5261

Radiometric calibration of the in-flight blackbody calibration system

C. Monte et al.

Title Page

Abstract

Introduction

Conclusions

References

Tables

Figures

◀

▶

◀

▶

Back

Close

Full Screen / Esc

Printer-friendly Version

Interactive Discussion



- Morozova, S. P., Parfentiev, N. A., Lisiansky, B. E., Melenevsky, U., Gutschwager, B., Monte, C., and Hollandt, J.: Vacuum Variable Medium Temperature Blackbody (VMTBB), *Int. J. Thermophys.*, 31, 1809–1820, 2010. 5259
- 5 Olschewski, F., Ebersoldt, A., Friedl-Vallon, F., Gutschwager, B., Hollandt, J., Kleinert, A., Monte, C., Piesch, C., Preusse, P., Rolf, C., Steffens, P., and Koppmann, R.: The in-flight blackbody calibration system for the GLORIA interferometer onboard an airborne research platform, *Atmos. Meas. Tech. Discuss.*, in preparation, 2013. 5253, 5256, 5257
- Prokhorov, A. V.: Monte Carlo method in optical radiometry, *Metrologia*, 35, 465–471, 1998. 5261
- 10 Prokhorov, A.: Blackbody emissivity modeling software STEEP320, available at: <http://www.virial.com/steep320.html> (last access: May 2013), 2013. 5261
- Riese, M., Ploeger, F., Rap, A., Vogel, B., Konopka, P., Dameris, M., and Forster, P.: Impact of uncertainties in atmospheric mixing on simulated UTLS composition and related radiative effects, *J. Geophys. Res.*, 117, 1–10, 2012. 5252
- 15 Riese, M., Friedl-Vallon, F., et al.: The GLORIA project: science, *Atmos. Meas. Tech. Discuss.*, in preparation, 2013. 5252, 5255
- Solomon, S., Rosenlof, K. H., Portmann, R. W., Daniel, J. S., Davis, S. M., Sanford, T. J., and Plattner, G.-K.: Contributions of Stratospheric Water Vapor to Decadal Changes in the Rate of Global Warming, *Science*, 327, 1219–1223, 2010. 5252
- 20 Ungermann, J., Blank, J., Lotz, J., Leppkes, K., Hoffmann, L., Guggenmoser, T., Kaufmann, M., Preusse, P., Naumann, U., and Riese, M.: A 3-D tomographic retrieval approach with advection compensation for the air-borne limb-imager GLORIA, *Atmos. Meas. Tech.*, 4, 2509–2529, doi:10.5194/amt-4-2509-2011, 2011. 5254

Radiometric calibration of the in-flight blackbody calibration system

C. Monte et al.

Table 1. Basic Parameters and Performance of the VLTBB.

Range of radiation temperature / °C	–173 to 177
Stability of PRT-temperature / mK	< 5 (after settling time)
Stability of radiation temperature / mK	< 30 (after settling time)
Normal effective emissivity	> 0.9997
Cavity diameter / mm	40
Cavity length / mm	250
Outer aperture diameter / mm	20
Shape of cavity bottom	75° outer cone
Overall dimensions of VLTBB diameter / mm × length / mm	200 × 450
Temperature differences along the cavity / mK	< 20 (after settling time)
Settling time (300 K up to 450 K) / min	< 30
Settling time (300 K down to 100 K) / min	< 60
Ambient temperature range for operation / °C	15 to 30
Temperature of the outer wall of the VLTBB / °C	15 to 40
Application	in vacuum chamber
Cavity wall coating	Aeroglaze Z306
Mass of VLTBB / kg	< 15

Title Page

Abstract

Introduction

Conclusions

References

Tables

Figures

◀

▶

◀

▶

Back

Close

Full Screen / Esc

Printer-friendly Version

Interactive Discussion

Radiometric calibration of the in-flight blackbody calibration system

C. Monte et al.

Table 2. Uncertainty components u ($k = 1$) of the radiation temperature of the VLTTB.

$t / ^\circ\text{C}$	Emissivity uncertainty (non-isothermal) u_e / K					PRT Noise	PRT Stability	PRT Calibration uncertainty
	4.8 μm	6.7 μm	9.9 μm	12.2 μm	14.1 μm	u_r / K	u_n / K	u_{Pt} / K
-80	0.025	0.009	0.009	0.009	0.034	0.001	0.064	0.015
-70	0.029	0.010	0.010	0.010	0.038	0.001	0.058	0.015
-60	0.033	0.011	0.011	0.011	0.042	0.001	0.053	0.015
-50	0.036	0.012	0.012	0.012	0.045	0.001	0.047	0.015
-40	0.040	0.013	0.013	0.013	0.050	0.001	0.042	0.015
-30	0.043	0.014	0.014	0.014	0.054	0.001	0.036	0.015
-20	0.047	0.015	0.015	0.015	0.058	0.001	0.031	0.015
-10	0.051	0.017	0.016	0.017	0.063	0.001	0.026	0.015
0	0.055	0.018	0.017	0.018	0.067	0.001	0.020	0.015
10	0.059	0.019	0.018	0.019	0.072	0.001	0.017	0.015
20	0.063	0.021	0.020	0.020	0.077	0.001	0.014	0.015
30	0.067	0.022	0.021	0.022	0.082	0.001	0.011	0.015
40	0.072	0.023	0.022	0.023	0.087	0.001	0.008	0.015
50	0.077	0.025	0.024	0.025	0.092	0.001	0.005	0.015
60	0.081	0.027	0.025	0.026	0.098	0.001	0.005	0.015
70	0.086	0.028	0.027	0.027	0.103	0.001	0.005	0.015
80	0.091	0.030	0.028	0.029	0.109	0.001	0.005	0.015

Title Page

Abstract

Introduction

Conclusions

References

Tables

Figures

◀

▶

◀

▶

Back

Close

Full Screen / Esc

Printer-friendly Version

Interactive Discussion



Radiometric calibration of the in-flight blackbody calibration system

C. Monte et al.

Table 3. Combined uncertainty u ($k = 1$) of the radiation temperature of the VLTBB.

$t / ^\circ\text{C}$	VLTBB, Combined uncertainty u / K				
	4.8 μm	6.7 μm	9.9 μm	12.2 μm	14.1 μm
–80	0.070	0.066	0.066	0.066	0.074
–70	0.067	0.061	0.061	0.061	0.071
–60	0.064	0.056	0.056	0.056	0.069
–50	0.061	0.051	0.051	0.051	0.067
–40	0.060	0.046	0.046	0.046	0.067
–30	0.058	0.042	0.042	0.042	0.067
–20	0.058	0.038	0.038	0.038	0.068
–10	0.059	0.034	0.034	0.034	0.069
0	0.060	0.031	0.030	0.031	0.072
10	0.063	0.030	0.029	0.030	0.076
20	0.066	0.029	0.029	0.029	0.080
30	0.070	0.029	0.028	0.029	0.084
40	0.074	0.029	0.028	0.029	0.089
50	0.078	0.030	0.029	0.029	0.094
60	0.083	0.031	0.030	0.030	0.099
70	0.088	0.032	0.031	0.032	0.105
80	0.093	0.034	0.033	0.033	0.110

Title Page

Abstract

Introduction

Conclusions

References

Tables

Figures

◀

▶

◀

▶

Back

Close

Full Screen / Esc

Printer-friendly Version

Interactive Discussion

Radiometric calibration of the in-flight blackbody calibration system

C. Monte et al.

Table 4. Maximum individual deviation of the measured radiation temperature from the fitted calibration curve (fourth-power polynomial) for each PRT with the corresponding standard uncertainty u of the radiation temperature measurement.

GBB-C			GBB-H		
PRT	max. Dev./K	u /K	PRT	max. Dev./K	u /K
S110	0.039	0.107	S210	0.010	0.103
S111	0.053	0.103	S211	0.019	0.085
S112	0.051	0.104	S212	0.014	0.095
S113	0.046	0.103	S213	0.013	0.066
S114	0.050	0.105	S214	0.020	0.063
S120	0.051	0.103	S220	0.009	0.067
S121	0.046	0.103	S221	0.019	0.068
S122	0.044	0.105	S222	0.013	0.085
S123	0.041	0.104	S223	0.016	0.067
S124	0.052	0.103	S224	0.019	0.089

Title Page

Abstract

Introduction

Conclusions

References

Tables

Figures

⏪

⏩

◀

▶

Back

Close

Full Screen / Esc

Printer-friendly Version

Interactive Discussion

Radiometric calibration of the in-flight blackbody calibration system

C. Monte et al.

Table 5. Maximum individual change of the fitted calibration characteristics for each PRT between the calibration campaigns in January 2012 and January 2013. Changes of less than 170 mK (corresponding to the target radiance uncertainty of 1 % of GLORIA measurements) are shown in regular typeface whereas changes of less than 500 mK (corresponding to the minimum radiance uncertainty requirement of 3 % of GLORIA measurements) are shown in italic typeface.

GBB-C		GBB-H	
PRT	max. Change /K	PRT	max. Change /K
S110	<i>0.197</i>	S210	0.053
S111	<i>0.228</i>	S211	0.129
S112	0.111	S212	0.101
S113	0.120	S213	0.064
S114	0.083	S214	0.108
S120	<i>0.231</i>	S220	0.089
S121	<i>0.251</i>	S221	0.144
S122	<i>0.360</i>	S222	<i>0.194</i>
S123	<i>0.205</i>	S223	0.155
S124	<i>0.178</i>	S224	0.141

Title Page

Abstract

Introduction

Conclusions

References

Tables

Figures

⏪

⏩

◀

▶

Back

Close

Full Screen / Esc

Printer-friendly Version

Interactive Discussion

Radiometric calibration of the in-flight blackbody calibration system

C. Monte et al.

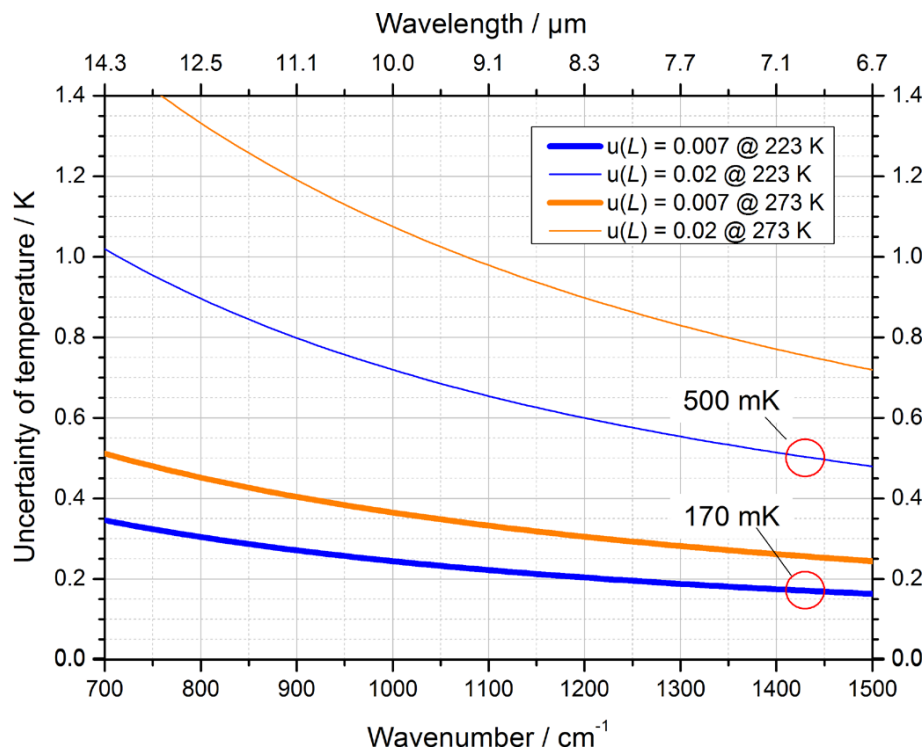


Fig. 1. Relationship between radiance uncertainty and radiation temperature uncertainty for the two extreme operation temperatures of the GBBs (-50°C and 0°C) and the two uncertainty levels 0.67% and 2% corresponding to GLORIAs target uncertainty of 1% and minimum requirement uncertainty of 3%.

[Title Page](#)[Abstract](#)[Introduction](#)[Conclusions](#)[References](#)[Tables](#)[Figures](#)[◀](#)[▶](#)[◀](#)[▶](#)[Back](#)[Close](#)[Full Screen / Esc](#)[Printer-friendly Version](#)[Interactive Discussion](#)

Radiometric calibration of the in-flight blackbody calibration system

C. Monte et al.

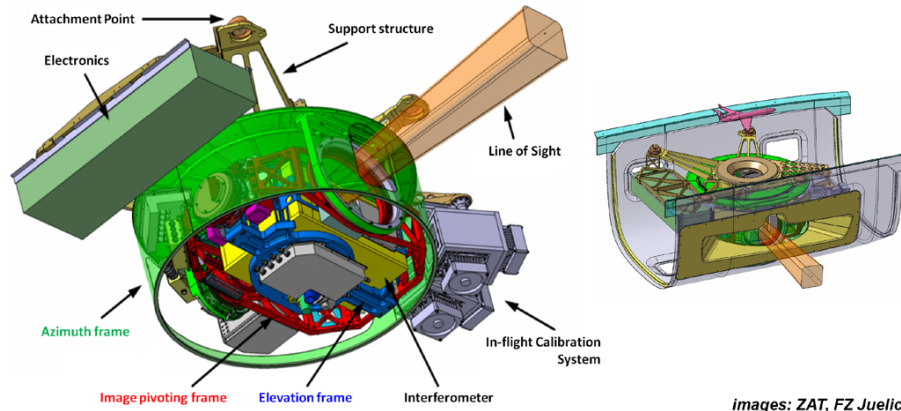


Fig. 2. Left: Gimbal-mounted GLORIA instrument with its in-flight calibration system; right: GLORIA in the belly pod of a research airplane.

[Title Page](#)[Abstract](#)[Introduction](#)[Conclusions](#)[References](#)[Tables](#)[Figures](#)[⏪](#)[⏩](#)[◀](#)[▶](#)[Back](#)[Close](#)[Full Screen / Esc](#)[Printer-friendly Version](#)[Interactive Discussion](#)

Radiometric calibration of the in-flight blackbody calibration system

C. Monte et al.

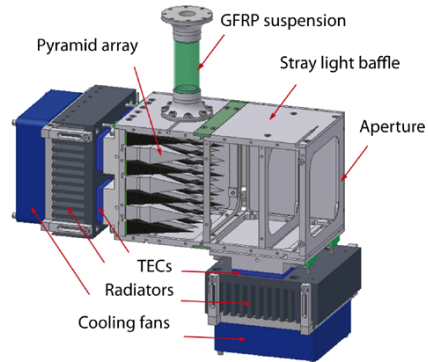


Fig. 3. Left: schematic diagram of a GLORIA blackbody; right: partly assembled prototype version of the pyramid array which forms the radiating optical surface of a GLORIA blackbody. Three different types of uncoated pyramids are noticeable. The position of platinum resistance thermometers in the pyramids and the base plate are marked in blue.

[Title Page](#)[Abstract](#)[Introduction](#)[Conclusions](#)[References](#)[Tables](#)[Figures](#)[◀](#)[▶](#)[◀](#)[▶](#)[Back](#)[Close](#)[Full Screen / Esc](#)[Printer-friendly Version](#)[Interactive Discussion](#)

Radiometric calibration of the in-flight blackbody calibration system

C. Monte et al.

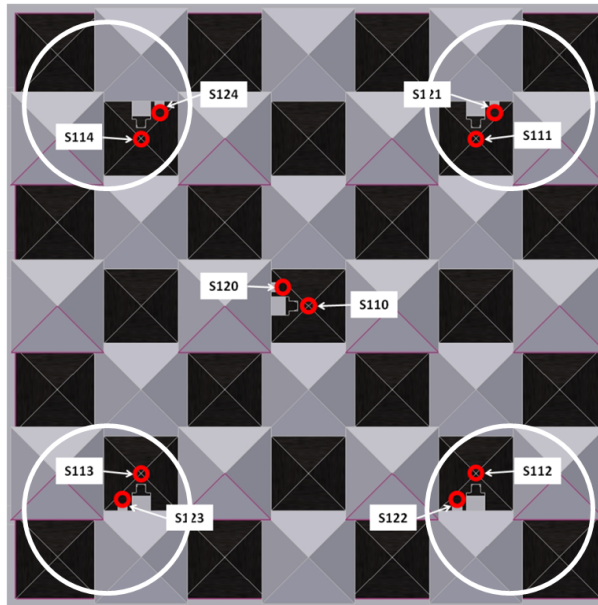


Fig. 4. Location of the 49 pyramids and the 10 platinum resistance thermometers (S110 to S114 and S120 to S124) on the radiating optical surface of a GLORIA blackbody. The white circles represent the field-of-view of the corner pixels of the GLORIA detector array.

Title Page

Abstract

Introduction

Conclusions

References

Tables

Figures

◀

▶

◀

▶

Back

Close

Full Screen / Esc

Printer-friendly Version

Interactive Discussion



Radiometric calibration of the in-flight blackbody calibration system

C. Monte et al.

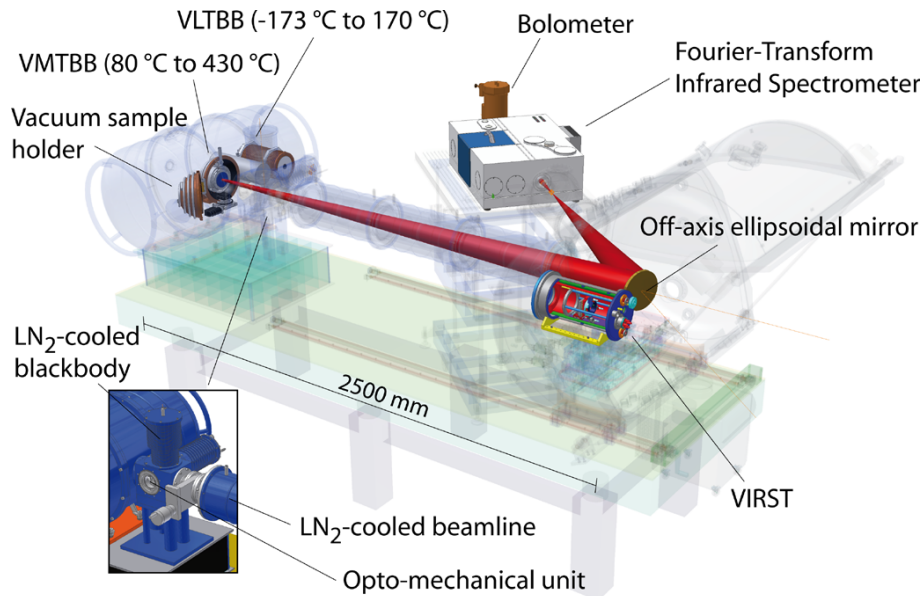


Fig. 5. Transparent view of the Reduced Background Calibration Facility to illustrate the position of the source chamber with the reference blackbodies VLTBB and VMTBB as well as the vacuum sample holder for emissivity measurements, the position of the opto-mechanical unit, with the folding mirrors, the chopper and the liquid-nitrogen-cooled reference blackbody, the position of the beam line and the position of the detector chamber with the radiation thermometer VIRST and an ellipsoidal mirror guiding the radiation into a Fourier transform spectrometer.

Title Page

Abstract

Introduction

Conclusions

References

Tables

Figures

◀

▶

◀

▶

Back

Close

Full Screen / Esc

Printer-friendly Version

Interactive Discussion

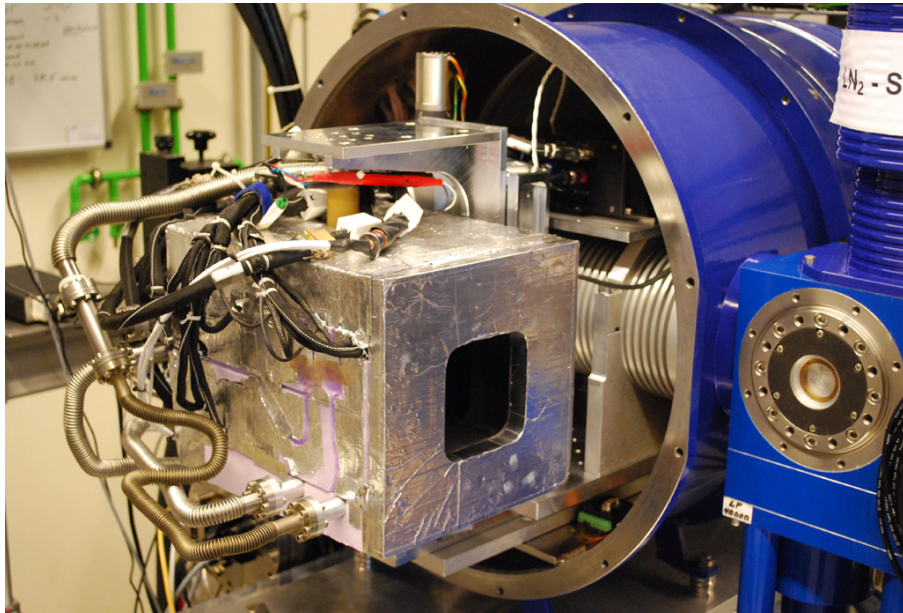


Fig. 6. View of the opened source chamber of the Reduced Background Calibration Facility. One of the GLORIA blackbodies is installed for calibration. To the right of the GLORIA blackbody, the reference blackbody VLTBB can be seen. Attached to the source chamber, the opto-mechanical unit with the liquid-nitrogen-cooled blackbody on top can partially be seen.

Radiometric calibration of the in-flight blackbody calibration system

C. Monte et al.

Title Page

Abstract

Introduction

Conclusions

References

Tables

Figures

◀

▶

◀

▶

Back

Close

Full Screen / Esc

Printer-friendly Version

Interactive Discussion

Radiometric calibration of the in-flight blackbody calibration system

C. Monte et al.

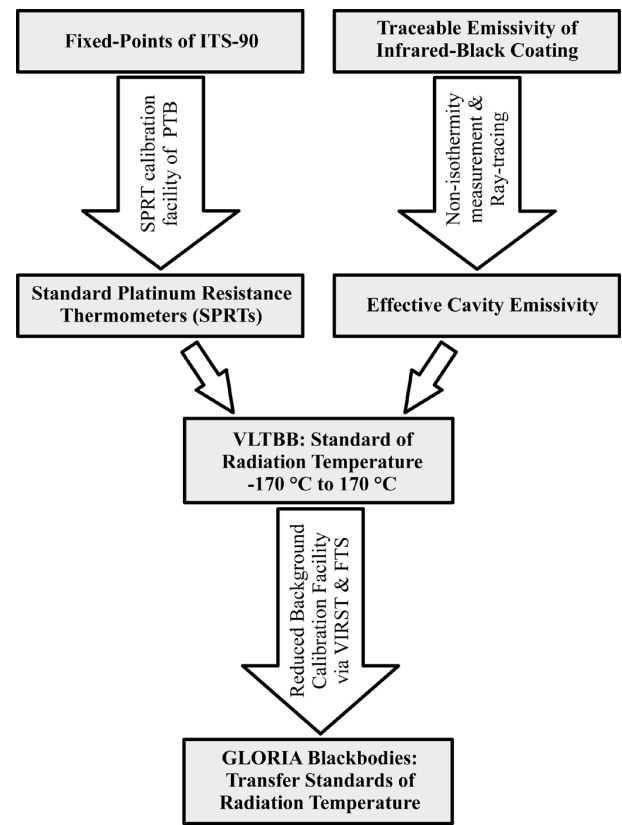


Fig. 7. Calibration chain diagram of the GLORIA Blackbodies.

[Title Page](#)

[Abstract](#) [Introduction](#)

[Conclusions](#) [References](#)

[Tables](#) [Figures](#)

[◀](#) [▶](#)

[◀](#) [▶](#)

[Back](#) [Close](#)

[Full Screen / Esc](#)

[Printer-friendly Version](#)

[Interactive Discussion](#)



Radiometric calibration of the in-flight blackbody calibration system

C. Monte et al.

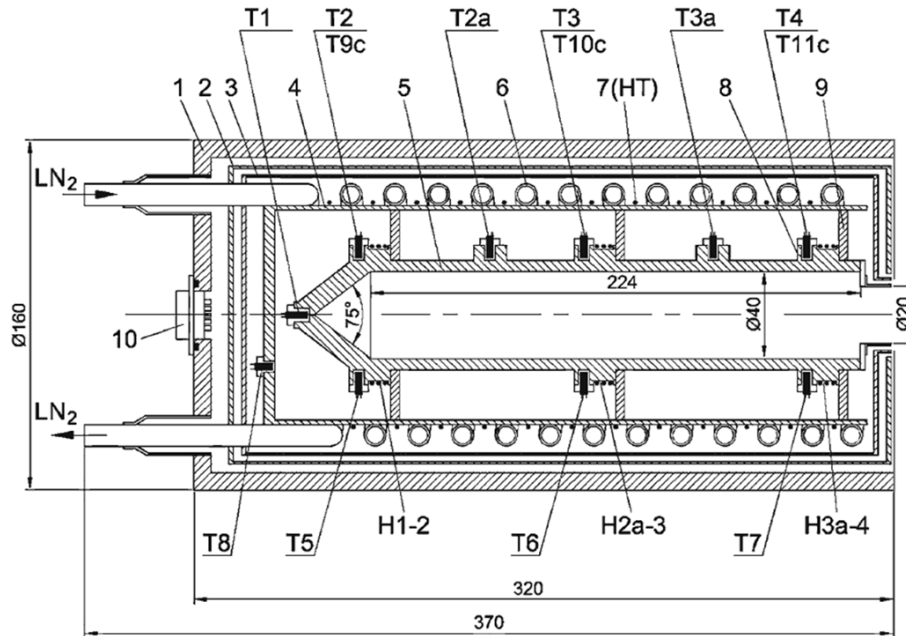


Fig. 8. Schematic diagram of the Vacuum Low Temperature Blackbody: 1 – body of the VLTBB, 2 – second radiation shield, 3 – first radiation shield, 4 – Cryo-shroud, 5 – cavity, 6 – cryo-shroud heat-exchanger, 7 – cryo-shroud heater, 8 – ring-shaped enhancement of the cavity, 9 – heat link, 10 – electrical connector.

Title Page

Abstract

Introduction

Conclusions

References

Tables

Figures

◀

▶

◀

▶

Back

Close

Full Screen / Esc

Printer-friendly Version

Interactive Discussion

Radiometric calibration of the in-flight blackbody calibration system

C. Monte et al.

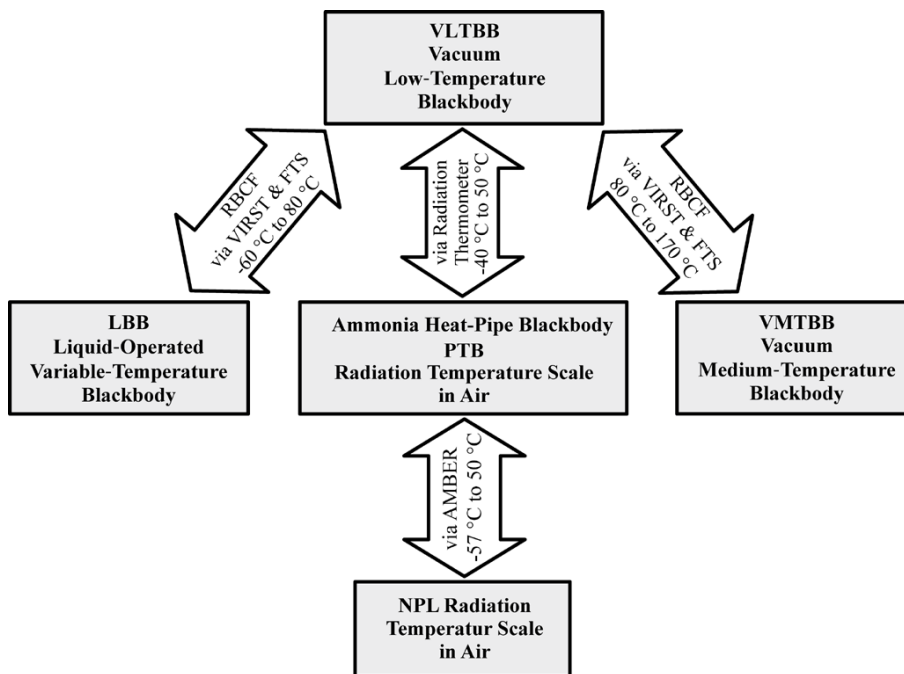


Fig. 9. Comparisons of the VLTTB with other radiation temperature standards in the context of the radiometric calibration of the GLORIA blackbodies.

Title Page	
Abstract	Introduction
Conclusions	References
Tables	Figures
◀	▶
◀	▶
Back	Close
Full Screen / Esc	
Printer-friendly Version	
Interactive Discussion	

Radiometric calibration of the in-flight blackbody calibration system

C. Monte et al.

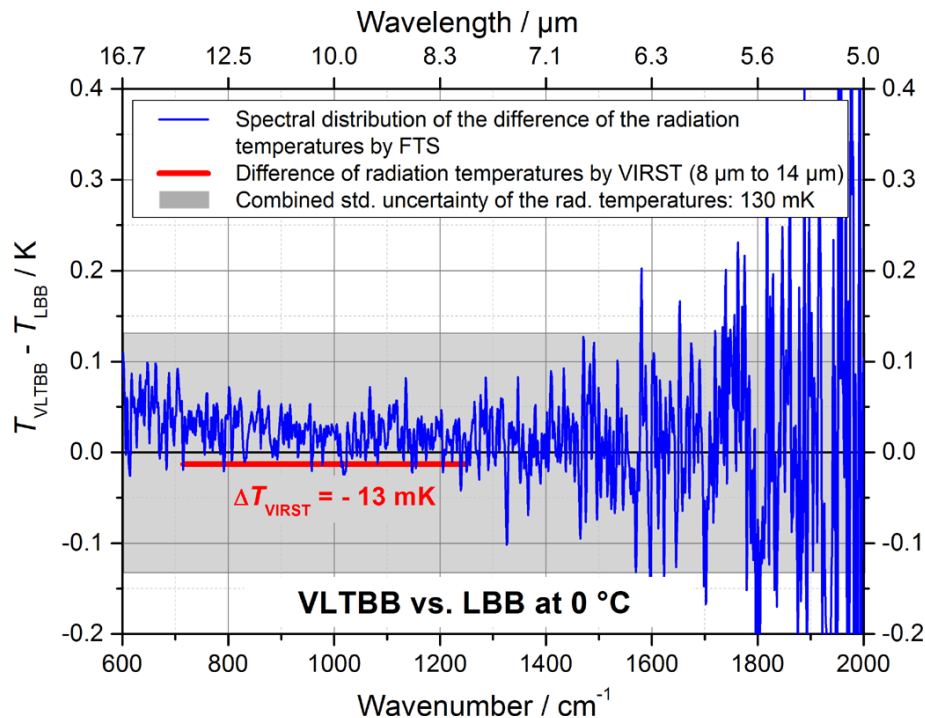


Fig. 10. Difference between the radiation temperatures of the VLTBB and the LBB at 0°C measured with the vacuum FTS (blue line) in the relevant wavelength range of the GLORIA instrument and with VIRST (red line) at the RBCF.

Title Page

Abstract

Introduction

Conclusions

References

Tables

Figures

◀

▶

◀

▶

Back

Close

Full Screen / Esc

Printer-friendly Version

Interactive Discussion

Radiometric calibration of the in-flight blackbody calibration system

C. Monte et al.

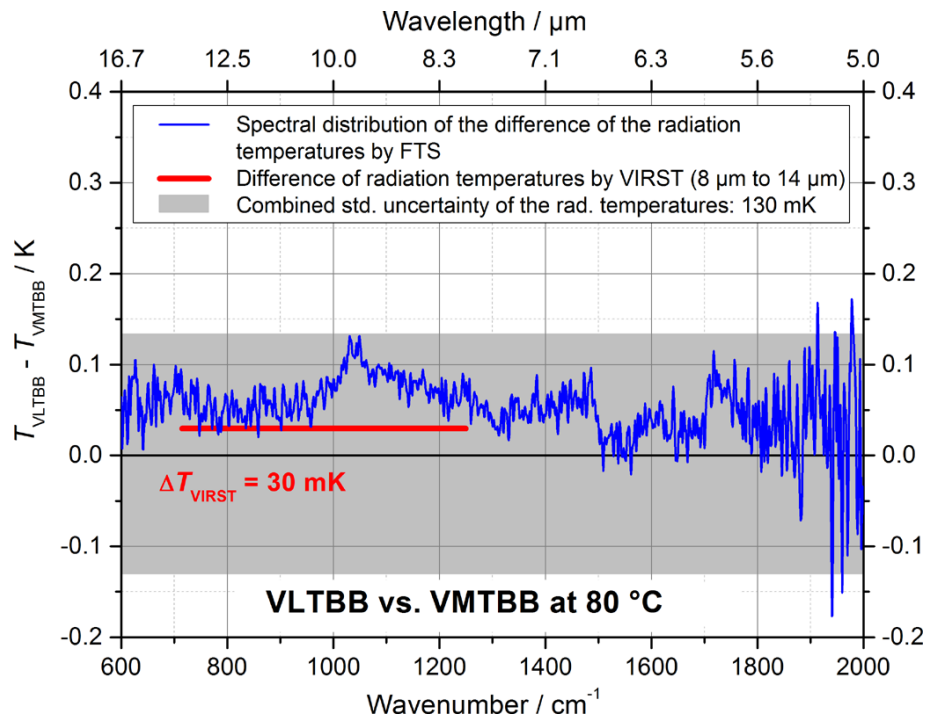


Fig. 11. Difference between the radiation temperatures of the VLTBB and the VMTBB at 80 °C measured with the vacuum FTS (blue line) in the relevant wavelength range of the GLORIA instrument and with VIRST (red line) at the RBCF.

[Title Page](#)
[Abstract](#)
[Introduction](#)
[Conclusions](#)
[References](#)
[Tables](#)
[Figures](#)
[⏪](#)
[⏩](#)
[◀](#)
[▶](#)
[Back](#)
[Close](#)
[Full Screen / Esc](#)
[Printer-friendly Version](#)
[Interactive Discussion](#)

Radiometric calibration of the in-flight blackbody calibration system

C. Monte et al.

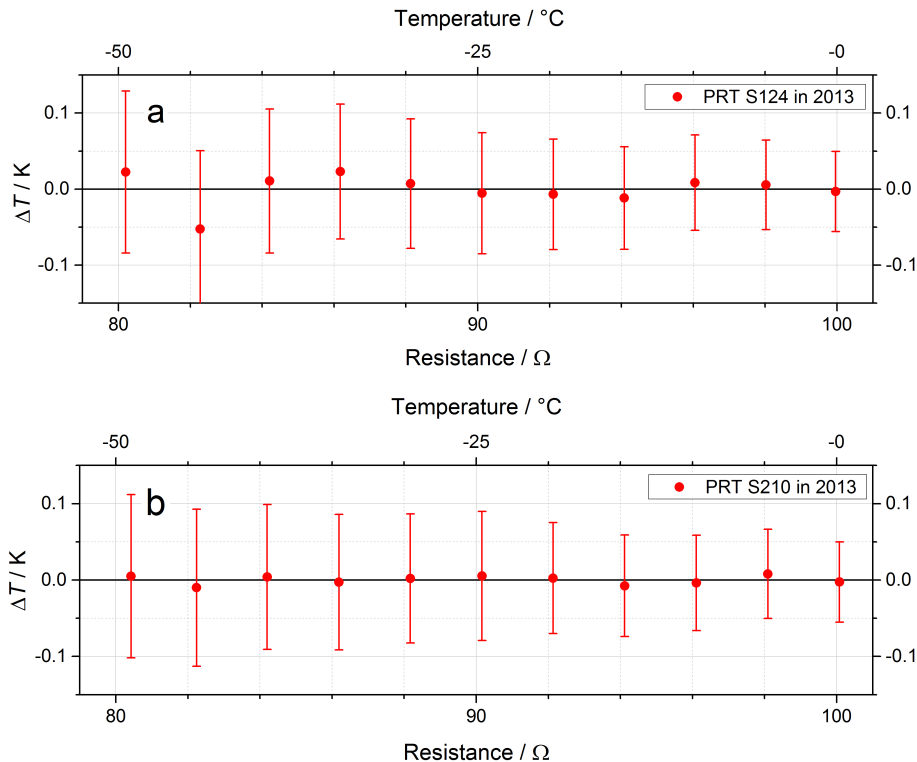


Fig. 12. Deviation (residuals) of the measured radiation temperature from the calibration curve at the measured resistance values (corresponding to temperature steps of 5°C from -50°C to 0°C) for two selected PRTs. **(a)** PRT S124 (GBB-C) which showed the largest deviation of a calibration point from the fitted calibration curve in the January 2013 calibration campaign, **(b)** PRT S210 (GBB-H) which showed the smallest deviation of all calibration points from the fitted calibration curve in the January 2013 calibration campaign.

Title Page

Abstract

Introduction

Conclusions

References

Tables

Figures

◀

▶

◀

▶

Back

Close

Full Screen / Esc

Printer-friendly Version

Interactive Discussion

Radiometric calibration of the in-flight blackbody calibration system

C. Monte et al.

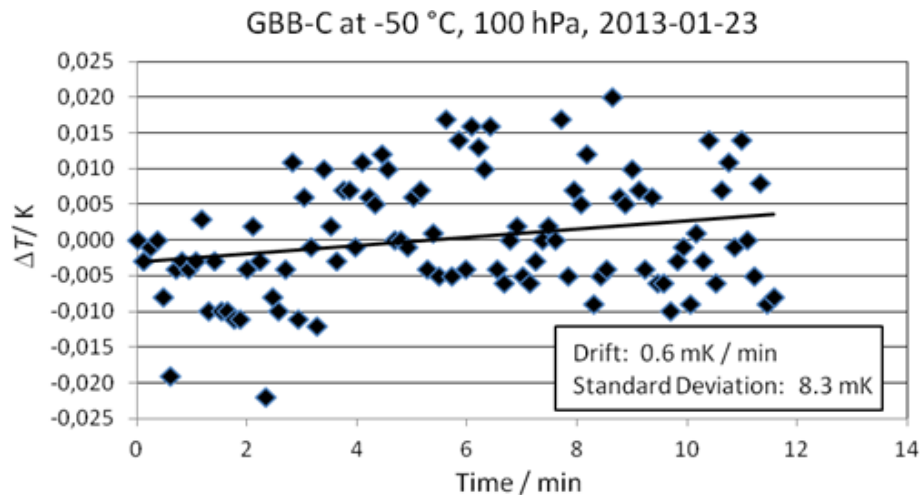


Fig. 13. Short-term stability of the radiation temperature of the GLORIA blackbody GBB-C at -50°C and 100 hPa observed in the middle of the optical surface.

Title Page

Abstract

Introduction

Conclusions

References

Tables

Figures

◀

▶

◀

▶

Back

Close

Full Screen / Esc

Printer-friendly Version

Interactive Discussion

Radiometric calibration of the in-flight blackbody calibration system

C. Monte et al.

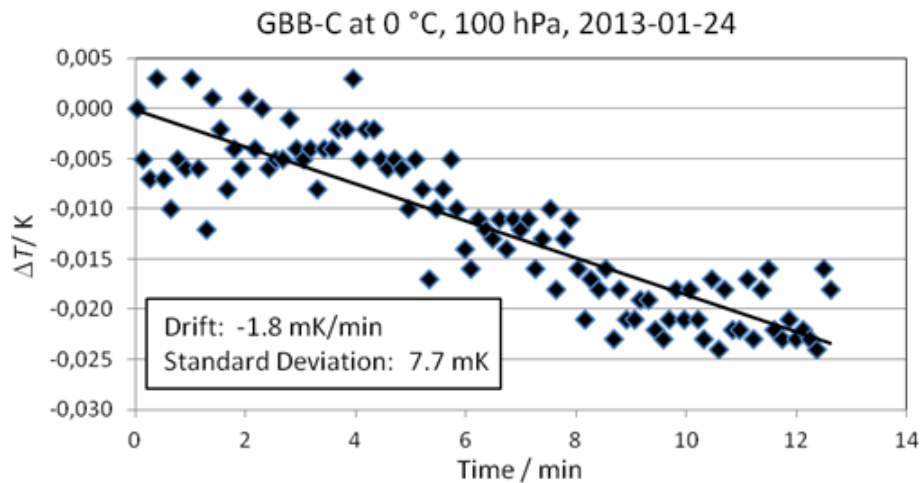


Fig. 14. Short-term stability of the radiation temperature of the GLORIA blackbody GBB-C at 0 °C and 100 hPa observed in the middle of the optical surface.

Title Page

Abstract

Introduction

Conclusions

References

Tables

Figures

◀

▶

◀

▶

Back

Close

Full Screen / Esc

Printer-friendly Version

Interactive Discussion

Radiometric calibration of the in-flight blackbody calibration system

C. Monte et al.

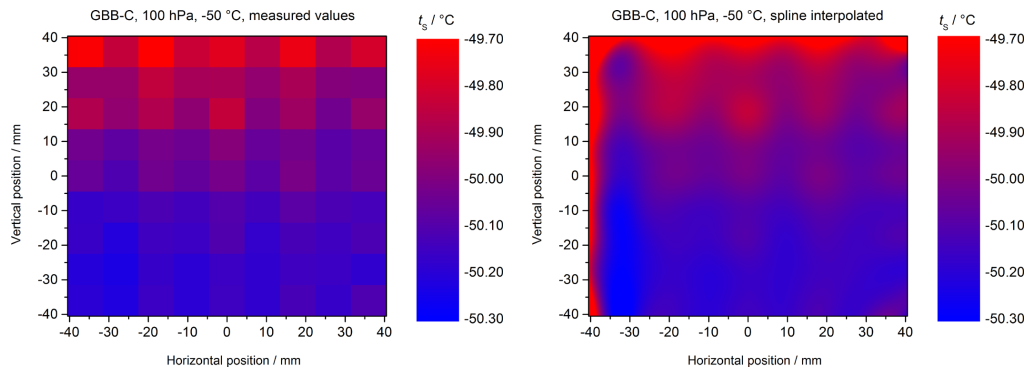


Fig. 15. The spatial distribution of the radiation temperature of the GLORIA blackbody GBB-C at a nominal temperature of -50 °C and 100 hPa. The field-of-view is 82 mm \times 82 mm. The measured data is shown on the left panel, the spline interpolated data on the right. The homogeneity is 132 mK (standard deviation).

[Title Page](#)[Abstract](#)[Introduction](#)[Conclusions](#)[References](#)[Tables](#)[Figures](#)[⏪](#)[⏩](#)[◀](#)[▶](#)[Back](#)[Close](#)[Full Screen / Esc](#)[Printer-friendly Version](#)[Interactive Discussion](#)

Radiometric calibration of the in-flight blackbody calibration system

C. Monte et al.

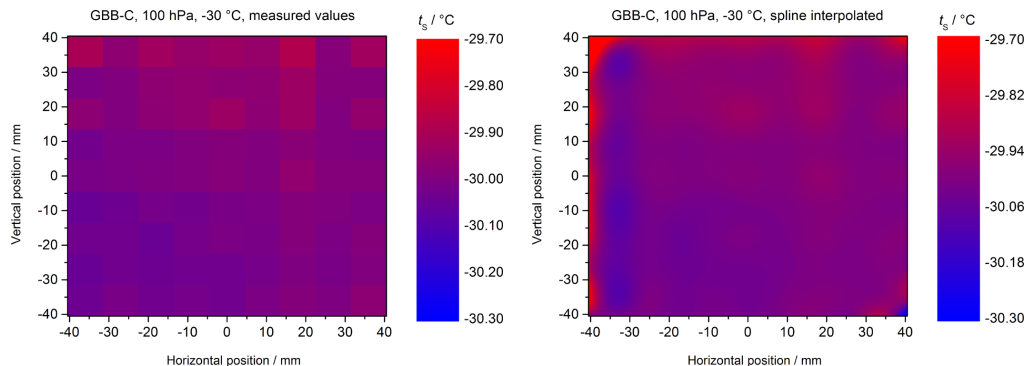


Fig. 16. The spatial distribution of the radiation temperature of the GLORIA blackbody GBB-C at a nominal temperature of -30 °C and 100 hPa. The field-of-view is $82\text{ mm} \times 82\text{ mm}$. The measured data is shown on the left panel, the spline interpolated data on the right. The homogeneity is 35 mK (standard deviation).

Title Page

Abstract

Introduction

Conclusions

References

Tables

Figures

⏪

⏩

◀

▶

Back

Close

Full Screen / Esc

Printer-friendly Version

Interactive Discussion



Radiometric calibration of the in-flight blackbody calibration system

C. Monte et al.

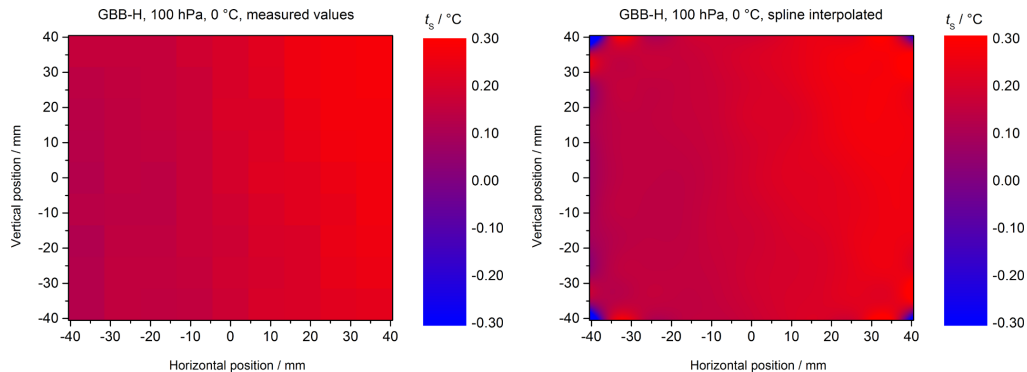


Fig. 17. The spatial distribution of the radiation temperature of the GLORIA blackbody GBB-H at a nominal temperature of 0 °C and 100 hPa. The field-of-view is 82 mm × 82 mm. The measured data is shown on the left panel, the spline interpolated data on the right. The homogeneity is 47 mK (standard deviation).

Title Page

Abstract

Introduction

Conclusions

References

Tables

Figures

◀

▶

◀

▶

Back

Close

Full Screen / Esc

Printer-friendly Version

Interactive Discussion

Radiometric calibration of the in-flight blackbody calibration system

C. Monte et al.

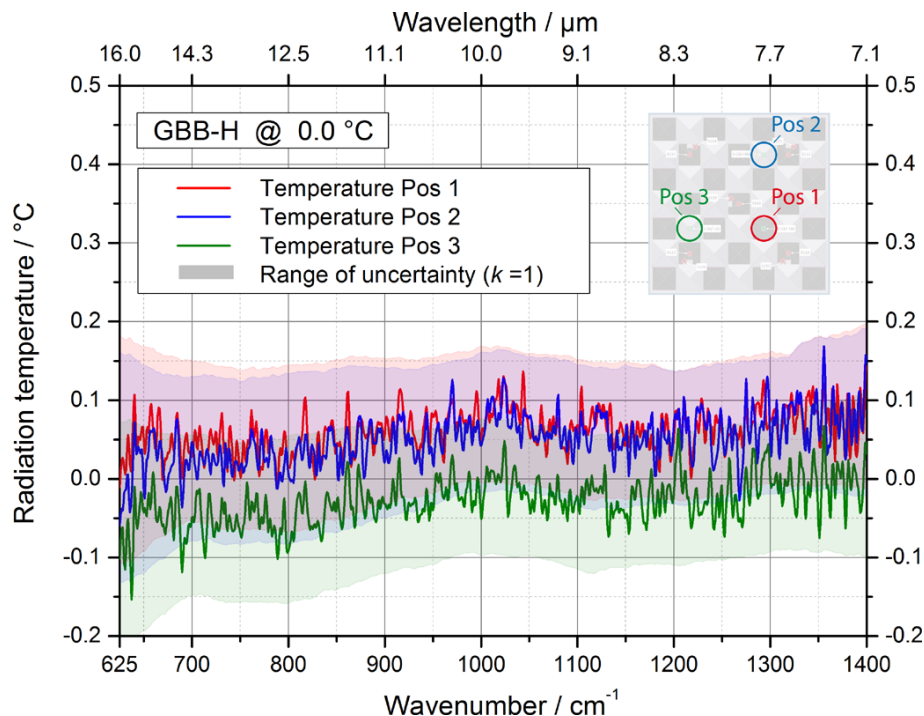


Fig. 18. The spectrally resolved radiation temperature of the GBB-H measured with the vacuum FTS at 0 °C and three different positions on the optical surface. The respective ranges of the measurement uncertainty are depicted as shaded areas. The three measurement areas on the optical surface of the GBB-H are shown as circles in the inset.

[Title Page](#)[Abstract](#)[Introduction](#)[Conclusions](#)[References](#)[Tables](#)[Figures](#)[◀](#)[▶](#)[◀](#)[▶](#)[Back](#)[Close](#)[Full Screen / Esc](#)[Printer-friendly Version](#)[Interactive Discussion](#)

Radiometric calibration of the in-flight blackbody calibration system

C. Monte et al.

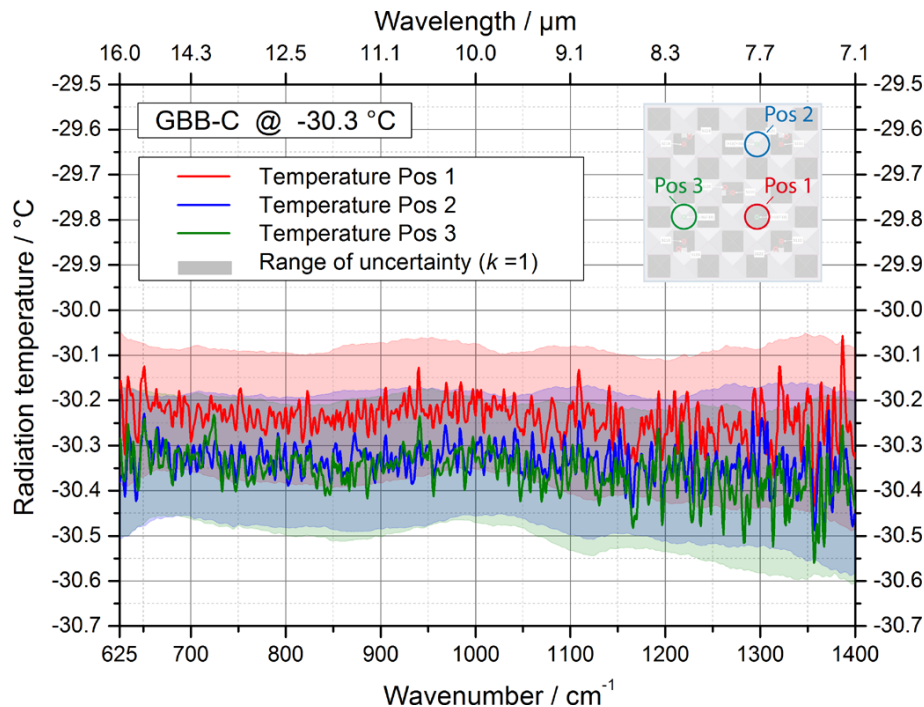


Fig. 19. The spectrally resolved radiation temperature of the GBB-C measured with the vacuum FTS at -30.3 °C and three different positions on the optical surface. The respective ranges of the measurement uncertainty are depicted as shaded areas. The three measurement areas on the optical surface of the GBB-C are shown as circles in the inset.

[Title Page](#)[Abstract](#)[Introduction](#)[Conclusions](#)[References](#)[Tables](#)[Figures](#)[◀](#)[▶](#)[◀](#)[▶](#)[Back](#)[Close](#)[Full Screen / Esc](#)[Printer-friendly Version](#)[Interactive Discussion](#)

Radiometric calibration of the in-flight blackbody calibration system

C. Monte et al.

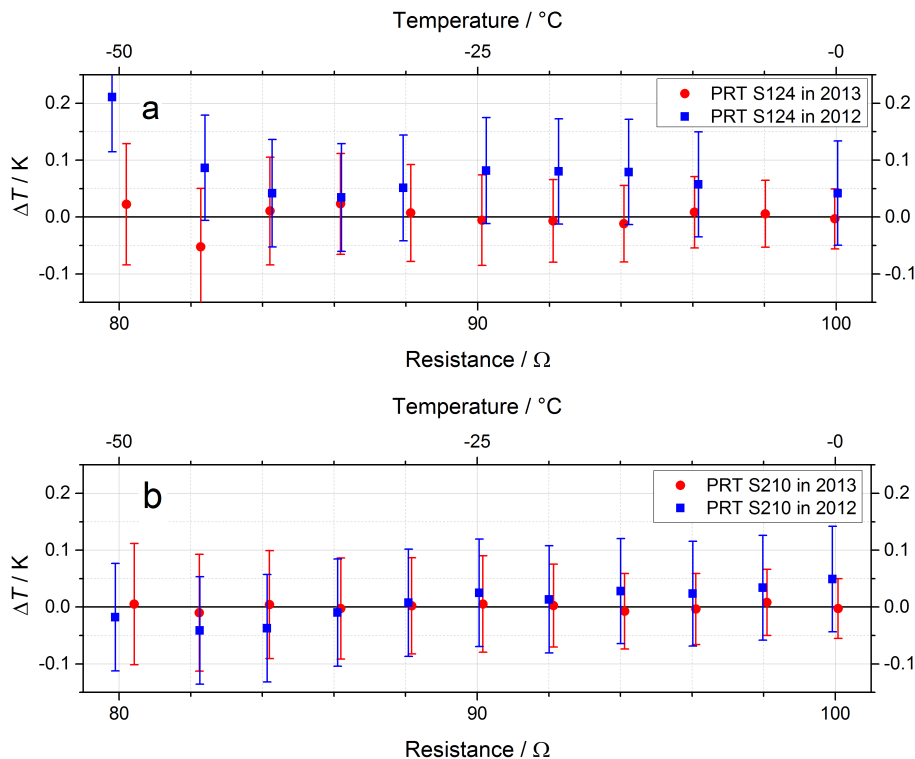


Fig. 20. The same calibration curves as in Fig. 12 are shown in red. Additionally, the deviations of the measured radiation temperatures of 2012 to the polynomial fit of 2013 are shown as a second curve in blue in each panel. **(a)** illustrates with PRT S124 a typical case of moderate changes whereas **(b)** illustrates with PRT S210 a typical case of small changes.

Title Page

Abstract

Introduction

Conclusions

References

Tables

Figures

◀

▶

◀

▶

Back

Close

Full Screen / Esc

Printer-friendly Version

Interactive Discussion